Proceedings of the
5th ASME/JSME Joint Thermal Engineering Conference
March 15-19, 1999, San Diego, California

AJTE99-6197

CYLINDRICAL PIN-FIN FAN-SINK HEAT TRANSFER AND PRESSURE DROP CORRELATIONS

Ning Zheng and R. A. Wirtz
Mechanical Engineering Department
University of Nevada, Reno
Reno, NV 89557

Keywords: Pin-fin fan-sink, Heat transfer correlation, Pressure drop correlation.

Abstract

New pressure drop / flow rate measurements coupled with a previously reported heat transfer database have resulted in new friction factor and heat transfer correlation equations for fan-driven impinging flow through square arrays of cylindrical cross-section pin-fins. The correlation equations include the effect of coolant flow rate, pin-fin density and pin-fin height. A comparison with a similar jet-driven impingement flow configuration shows that the heat transfer / pressure drop characteristics of the two flow configurations are fundamentally different. When the same arrays are compared at the same coolant flow rate, the fan-driven configuration will result in a lower pressure drop and heat transfer rate. An analysis shows that different optimal pin-fin configurations (fin height and fin density) result, depending on the design criteria imposed on the flow.

Nomenclature

A	Heat transfer area
a	Fin height
C_p	Coolant specific heat
$C_{\Delta P}$	Dimensionless pressure rise
D	Fin area density
d	Fin hydraulic diameter
d_f	Fan shroud diameter
d_h	Fan hub diameter
f	Heat sink friction factor
k	Coolant thermal conductivity
L	Heat sink footprint size
Nu	Nusselt number
n	Number of fins
Pr	Coolant Prandtl number
p	Fin pitch
Q	Flow rate
Re	Heat sink Reynolds number
U	Fin heat transfer coefficient
ΔP	Pressure change
μ	Coolant viscosity
ρ	Coolant density
ω	Fan speed

Introduction

For low-end electronic systems where air-cooling is the preferred thermal control method, “fan-sinks” are employed to supplement system fans in the cooling of sensitive or high-power components. A typical fan-sink consists of a small axial flow fan attached to the top of a heat sink with the heat sink base in thermal contact with the electronic component. The heat sink is usually an extruded, cast or forged form with either plate fins or an array of pin fins attached to its base plate. The fan-driven coolant flow impinges on the heat sink from above and exits the array in cross-flow.

For a given fan operating at its nominal speed, the heat sink fin geometry determines the overall thermal conductance of the assembly, UA. For example, a decrease in fin density decreases the heat transfer surface area, A, while the flow rate through the fin array, Q, increases. This tends to increase the fin heat transfer coefficient, U. On the other hand, an increase in fin density results in the opposite effect, U decreases while A increases. The same type of performance trade-off will occur with variations in fin height. Obviously, there will be an optimal fin configuration (fin density and height) that maximizes the UA-product. Wirtz and Zheng [1998] have described a methodology for determining this optimum. Proper design requires knowledge of both the assembly fan characteristic, and the heat transfer / pressure drop characteristic of the heat sink.

Fan characteristic curves (ΔP vs. Q) are generally available from the manufacturer, or they may be approximated using a generic fan performance correlation such as the one developed by Wirtz and Zheng [1998]. On the other hand, heat transfer / pressure drop correlations for heat sinks with a fan-driven impinging flow are not generally available in the technical literature.

Wirtz et al. [1997] measured the per-pin heat transfer coefficient of model fan-sink assemblies consisting of a small axial flow fan that impinges air on a square array of

cylindrical cross section pin-fins. They found that pins immediately under the fan blades had the highest heat transfer coefficient. Pins under the fan hub had the lowest (approximately 70% less than the heat transfer coefficient of pins under the fan blades). They developed a correlation for the overall fan-sink heat transfer coefficient as a function of the pressure rise induced by the fan. However, they did not measure the fan discharge, so they do not report the relation between fan induced pressure rise and coolant flow rate through their arrays.

Sparrow and Larson [1982] studied heat transfer in pin-fin arrays exposed to a jet-impinging flow. They measured the per-pin mass transfer coefficient using the naphthalene sublimation technique. They found that the Sherwood number for pins near the edge of the array are properly correlated by the exit velocity of the coolant while those near the center of the array correlate with the impingement velocity. Sparrow and Larson developed four different correlations for pin-fins in four regions of the array: corner pin-fins, edge pin-fins, central pin-fins, and the remaining pin-fins in the interior of the array. They also found that the friction factor for flow through their arrays is independent of flow rate.

Jet-impinging flows appear to be fundamentally different from fan-induced flows. For one thing, the coolant flow does not contain fan-induced swirl. Furthermore, the fan-induced flow configuration includes blockage from the fan's hub, which amounts to approximately 27% of the fan's frontal area. This gives rise to a significant reduction in the heat transfer coefficient of those pin-fins immediately below the hub. Therefore, application of jet-impingement correlations to the fan-driven problem will probably induce unacceptable error.

In this study, we consider the same cylindrical pin-fin arrays as were considered by Wirtz and co-workers. We measure the pressure rise across the fan as a function of fan speed. The fan characteristic equation is used to determine the flow rate through the assembly. A new correlation for the assembly friction factor is developed, and this can be combined with the Nusselt number correlation reported by Wirtz et al. [1997] to assess fan-sink assembly performance. These results are compared to jet-impingement correlations developed by Sparrow and Larson [1982]. Methods for optimizing the array configuration for given flow conditions are discussed.

Dimensional Analysis

Consider a heat sink having pin-fins arranged in an $(n \times n)$ square array of edge-length, L. The pins have diameter, d, and height, a. An axial flow fan, having fan shroud diameter, d_f, and hub diameter, d_h, impinges air normal to the fin array with the flow exiting in the radial direction. Assume the pressure drop of the fan-driven impinging flow through the array is a function of the following parameters:

$$\Delta P = fct_1(Q, d, a, L, D, D_{\max}, r, m, d_f, d_h) \tag{1}$$

where ρ and μ are the density and viscosity of air, and the area fin-density, D, is defined as

$$D = n^2 \frac{p}{4}\left(\frac{d}{L}\right)^2 \tag{2}$$

Note, for arrays of circular cross-section pin-fins, there is a maximum fin density, $D_{max} = \pi/4$, where adjacent pin-fins touch each other, thus choking off flow through the array. Under these conditions, $n_{max}d = L$, where n_{max} is an integer.

Dimensional analysis gives,

$$f = fct_2(\mathrm{Re}, \frac{d}{L}, \frac{a}{L}, D, D_{\max}, \frac{d_f}{L}, \frac{d_h}{d_f}) \tag{3}$$

where $f = \dfrac{\Delta P L^4}{r \cdot Q^2}$ is the friction factor and $\mathrm{Re} = \dfrac{r \cdot Q}{mL}$ is the heat sink Reynolds number.

Experiments

The purpose of the testing is to obtain the fan-driven flow rate through the array, Q, and the corresponding pressure drop, ΔP, as functions of fan speed, ω, for various cylindrical-pin-fin array configurations. The resulting Q - ΔP relationship gives Eq. (3) directly. Then, this data is combined with the U - ΔP data of Wirtz et al. [1997] to give a U – Q heat transfer correlation that can be used to assess (fan + heat sink) thermal performance.

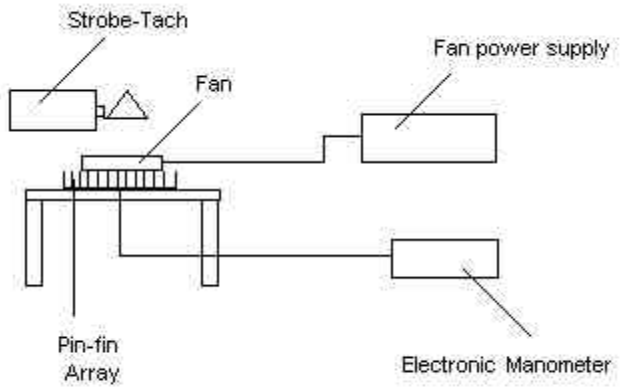

Fig. 1 Model fan-sink test rig

Test apparatus. A schematic of the test rig is shown in Figure 1. The pin-fin array is exposed to a fan-driven flow as found in a fan-sink assembly. A small axial-flow fan (d_f = 52 mm, d_h = 27 mm) drives the laboratory air, which impinges vertically on the fin array and exits the array horizontally. The flow rate Table 1 Geometric characteristics of cylindrical pin-fin arrays (L=63.5mm, d=3.17mm)

Array	n	a(mm)	p(mm)	a/L	p/d	D
a	10	10	6.70	0.157	2.114	0.196
b	10	15	6.70	0.236	2.114	0.196
c	10	20	6.70	0.315	2.114	0.196
d	14	10	4.64	0.157	1.464	0.385
e	14	15	4.64	0.236	1.464	0.385
f	14	20	4.64	0.315	1.464	0.385

through the array is controlled by varying the fan speed. The fan speed is controlled by a DC power supply, and it is measured with a strobe light with an accuracy of ±100 rpm. A 0.5 mm diameter pressure port is embedded at the center of the pin-fin array. The pressure drop across the array is measured using an electronic manometer having an accuracy of ±0.09 mm H_2O.

Array geometry. All pin-fin arrays tested are the same ones considered in the previous work [Wirtz et al., 1997]. Each array, with L = 63.5 mm on edge, consists of polished aluminum pin-fins (d = 3.17 mm = 1/8 inch) mounted to a fiberglass base. Table 1 summarizes the geometric characteristics of the pin-fin arrays considered in the test, where $p = \dfrac{L-d}{n-1}$ is the fin pitch.

Six different cylindrical pin-fin arrays are considered with the fin pitch-to-diameter ratio (p/d) = 1.464 and 2.114 and dimensionless fin-height (a/L) ranging from 0.157 to 0.315.

Array pressure drop. Figure 2 shows the test results for these six arrays for various fan speeds. The figure shows that the pressure drop across the assembly is increased as the fan's rotational speed increases. At fixed fan speed, the pressure drop is increased with a reduction of fin height at fixed fin density. The pressure rise is also increased with an increase in fin density at fixed fin height.

Coolant flow rate, Q. It is difficult to directly measure the flow rate, Q, since the performance of these small fans is sensitive to the presence of even a small flow transducer. However, the flow rate through the fan is equal to the flow rate through the heat sink, and the pressure rise across the fan is equal to the pressure drop across the heat sink. Therefore, we can use the measured fan speed (ω) and pressure rise across the fan (ΔP), together with the manufacturer supplied fan characteristic curve, shown in dimensionless form in Figure 3, to determine the flow rate (Q). Note the fan curve of Figure 3 is plotted in universal coordinates. In Fig. 3, the symbols designate the operating points of the various Q - ΔP

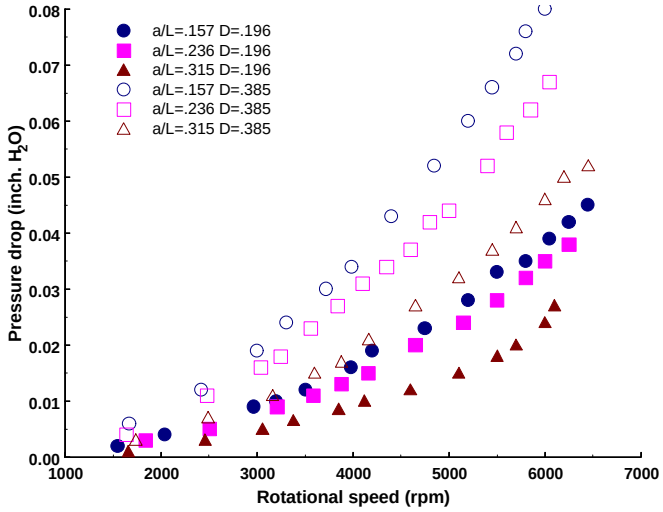

Fig. 2 Test results of pressure drop vs. fan rotational speed

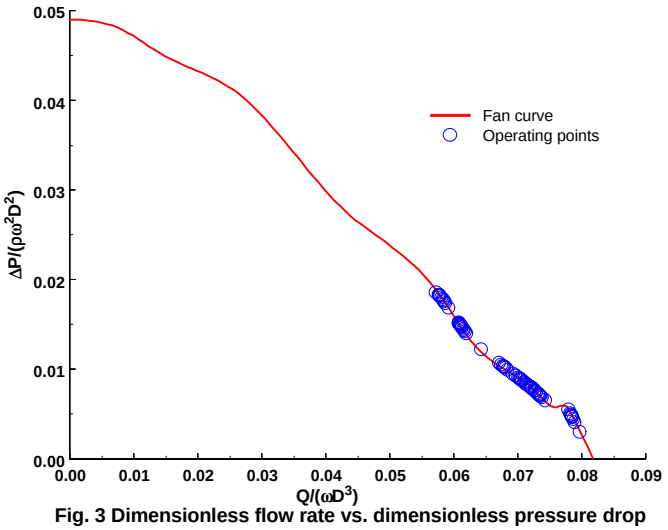

Fig. 3 Dimensionless flow rate vs. dimensionless pressure drop

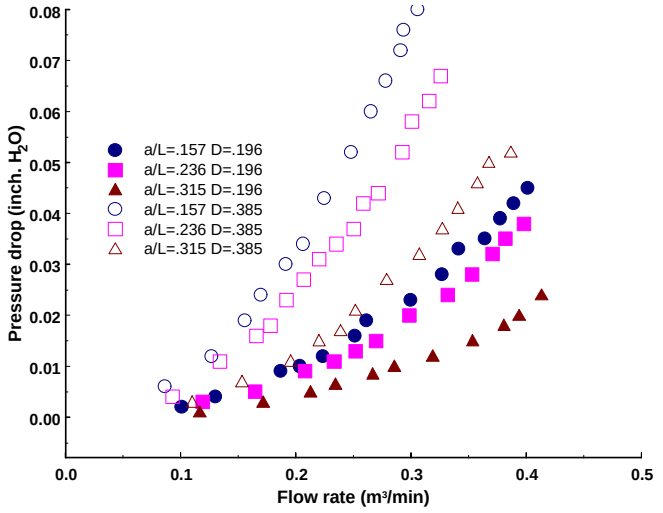

Fig. 4 Extended results of flow rate vs. pressure drop through heat sink

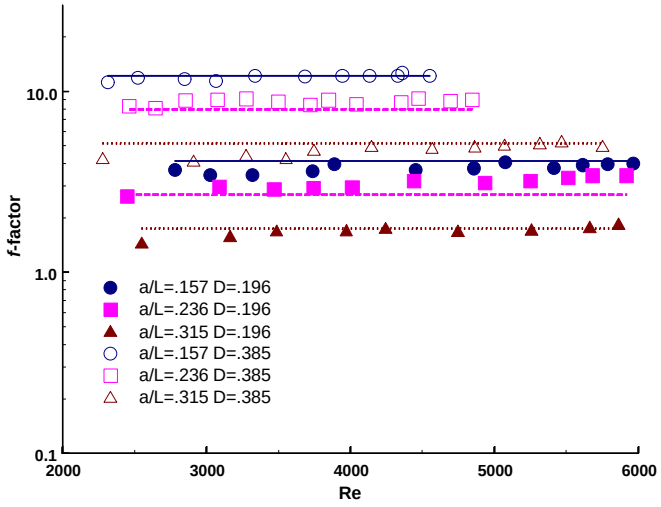

Fig. 5 Relation of *f* factor and Re

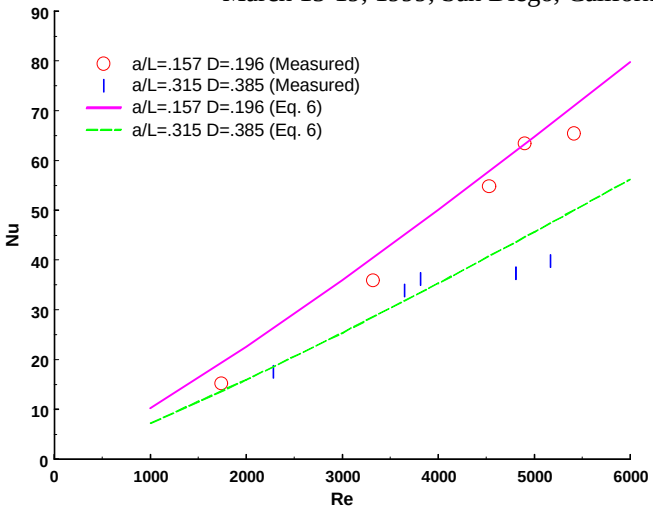

Fig. 6 Comparison of measurements with Eq. (6)

measurements reported in this paper, obtained at various fan speeds. Figure 4 shows the pressure drop data plotted as a function of flow rate, Q, determined using this algorithm. A Monte Carlo error simulation shows that the maximum error in Q is ±7% [Zheng, 1998].

Friction Factor Correlation. Figure 5 shows the ΔP – Q correlation plotted in terms of friction factor, *f*, and Reynolds number, Re. An error propagation analysis shows that the 99% confidence-level expected error in *f* ranges from ±34% at the lowest Reynolds number to less than 10% when Re > 5200. The 99% confidence level expected error in Reynolds number is less than ±7%. The data show that *f* is only weakly dependent on Re, so following Sparrow and Larson [1982], we neglect the dependence of *f* on Re in Eq. (3). Furthermore, we expect that *f* is inversely proportional to (D_{max} – D) since, for any applied pressure drop, the flow rate through the array must approach zero as D approaches D_{max}. Finally, all measurements reported here are for d/L = 0.05 and d_f/L = 0.819, and d_h/d_f = 0.519.

Under these conditions, Eq. (3) reduces to

$$f = fct_3\left(\frac{a}{L}, D_{\max} - D\right) \tag{4}$$

We find that the present data set is best correlated with the following equation

$$f = 2.202 \cdot e^{-5.457\frac{a}{L}} \cdot \left[\frac{p}{4} - D\right]^{-2.814} \tag{5}$$

Equation (5), shown as horizontal lines in Fig. 5, reproduces the present data with an rms deviation of ±14.6%[1].

[1] If the Reynolds number effect is included in the regression analysis, $f \sim \mathrm{Re}^{0.2}$, inclusion of this effect in Eq. (3) reduces the rms deviation of the data about the resulting power-law correlation equation to ±14.1%.

Heat Transfer Correlation. Wirtz et al. [1997] measured the heat transfer coefficient for arrays having D = 0.127, 0.196 and 0.385, with a/L = 0.157, 0.236 and 0.315. They correlated their heat transfer data in terms of fan-applied pressure rise,

$$Nu = 7.12\times10^{-4} C_{\Delta P}{}^{0.574} \left(\frac{a}{L}\right)^{0.223} \left(\frac{p}{d}\right)^{1.72} \tag{6}$$

where

$$C_{\Delta P} \equiv \frac{rL^2\Delta P}{m} = f\,\mathrm{Re}^2 \tag{7}$$

is the dimensionless pressure rise (drop) across the fan (array), and p/d is the fin pitch–to-diameter ratio. We can combine Eqs. (5) – (7) to form a correlation for Nusselt number as a function of Reynolds number, fin height and fin density, Nu(Re, a/L, D). Figure 6 compares measurements for Cases a, and f of Table 1 with the predictions of Eqs. (5) – (7). The system, Eqs. (5) – (7), reproduces the data that generated it with an rms deviation of ±9.8%. Wirtz and coworkers report that the 99% confidence level expected error in Nusselt number is less than ±12%.

Discussion of Results

Comparison with Jet-Driven Flow. In their study of jet-driven impingement heat transfer, Sparrow and Larson [1982] considered pin-fin arrays with $0.186 \le \frac{a}{L} \le 0.992$, $0.061 \le D \le 0.193$ and $0.046 \le \frac{d}{L} \le 0.083$. In the following, we compare our observations regarding fan-driven impingement with their work.

Sparrow and Larson found that the friction factor is essentially independent of the Reynolds number. We have also

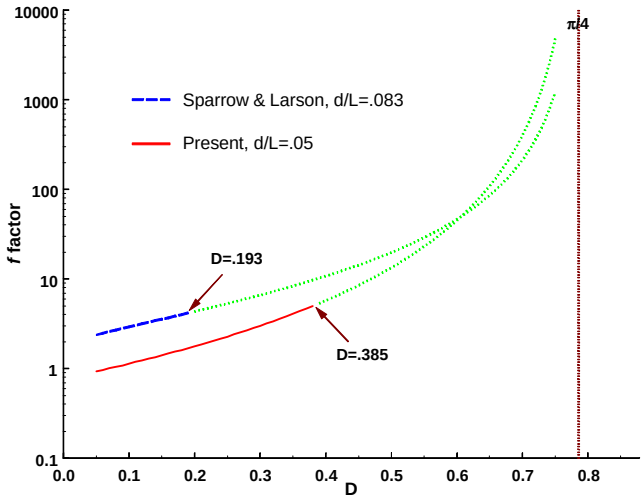

Fig. 7 Comparison of two *f*-factor correlation equations

found this to be the situation with a fan-driven impinging flow. Figure 7 compares the two correlation equations where $f(\frac{a}{L}, D)$ is plotted versus fin density, D. The jet-driven flow correlation is plotted as a dash-dash line up to D = 0.193, and then as a dot–dot line for D > 0.193, where we are extending it outside of the range of Sparrow and Larson's experimental work. The fan-driven flow correlation is extended in a similar manner. The figure shows that *f*(jet-driven) is approximately 65% higher than *f*(fan-driven) at D = 0.06, and the difference decreases to zero at D = 0.62. We believe the principal reason for the difference between the two results is that pin-fins beneath the fan-hub do not contribute to the overall pressure drop across the array since the coolant is essentially quiescent in this region. It is interesting that both correlation equations have $f \rightarrow \infty$ as $D \rightarrow D_{max}$, signifying that the flow through the array is choked-off as the fin density increases toward the maximum.

Sparrow and Larson developed per-pin Sherwood number correlation equations for four regions of the array. The corresponding Nusselt number is obtained by multiplying the Sherwood number by $\Pr^{1/3} = 0.632$. The overall Nusselt number for the array is obtained by weighted summation of the per-pin Nusselt numbers. For an n × n array, this may be implemented by combining corner-pins [4] with edge-pins [4(n-2)], central pins [a 4 × 4 array], and the remaining pins [$n^2 - 4n - 12$].

A comparison of the two correlations shows that Nu(jet-driven) is generally greater than Nu(fan-driven). When D = 0.2, the difference is approximately 10% at Re = 1000, and it increases to approximately 37% at Re = 10,000. This is, again, due to blockage of the coolant flow by the fan hub, causing the central pin-fins of the array to not effectively participate in the heat transfer process. Figure 8 compares the two correlation equations as a function of D at Re = 5000 and a/L = 0.3. Dot-dot lines show extensions to each correlation

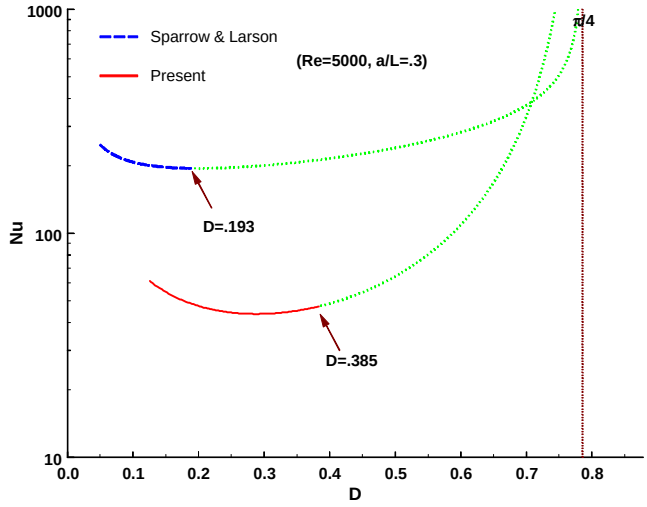

Fig. 8 Comparison of two Nu correlation equations

outside the range of data that generated it. Both correlation equations show Nu initially decreasing with an increase in D (over their range of applicability). This result appears to be somewhat counter intuitive. The flow cross section area decreases as the fin density is increased. As a result, the local flow velocity inside of the array will increase, and one would expect that this would lead to an increase in the heat transfer coefficient. Both correlation equations display the expected behavior at larger values of D, as $D \rightarrow D_{max}$: Nu(jet-driven) is seen to increase when D > 0.2, and Nu(fan-driven) increases when D > 0.3.

Implications to Fan-Sink Design. At fixed flow rate, U increases with a/L, and as shown in Fig. 8, it passes through a minimum as D varies. The heat transfer surface area

$$\frac{A}{L^2} = \left(1 + 4D\frac{a}{d}\right) \tag{8}$$

increases with both fin density and fin height. Due to these trade-offs in the magnitudes of U and A with changes in a/L and D, we expect that there may be an optimal heat sink geometrical configuration that maximizes the UA product for a given flow condition. Consider the case where we wish to determine a/L and D that maximizes UA for a constant pressure drop application. Under these conditions, the dimensionless pressure rise $C_{\Delta p} = f\,\mathrm{Re}^2$ is a constant in Eq. (6). For large n, the fin pitch-to-diameter ratio, p/d, is proportional to $D^{-0.5}$, so $Nu \propto \left(\frac{a}{L}\right)^{0.223} D^{-0.86}$. For fixed ΔP and D, it is clear that the product UA increases with a/L. However, at fixed ΔP and a/L, $UA \propto D^{-0.86}\left(1 + 4D\frac{a}{d}\right)$, so depending on the magnitude of a/d, UA might increase or decrease with increased fin density. Figure 9 shows a sample calculation where the thermal capacity is plotted versus fin

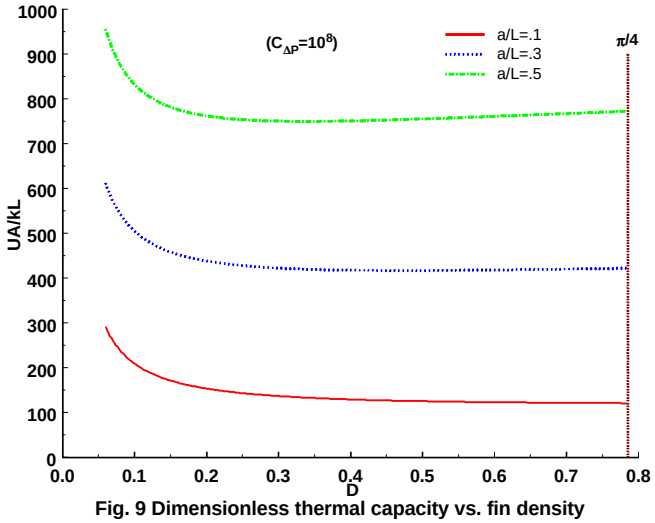

Fig. 9 Dimensionless thermal capacity vs. fin density

density for $C_{\Delta P} = 10^8$, a typical value for these small-fan applications. Results are plotted for three dimensionless fin heights: a/L = 0.1, 0.3 and 0.5. The figure shows that the best thermal performance is obtained when the fin density is minimized. Of course, at fixed ΔP, the flow rate through the array will increase as D is reduced, so there may be some practical limitations on the lower bound of the magnitude of D. For the case shown in Fig. 9, the Reynolds number ranges to 17,500 (at a/L = 0.5, D = 0.06).

A repeat of this analysis under a constant flow rate constraint (Re = 5000) will result in UA having a minimum at $D \cong 0.2$, followed by a steady increase as D approached D_{max}. Analysis that mates a small axial flow fan to a heat sink will result in other optimal array geometrical configurations, depending on the characteristics of the fan mated to the fin array.

Conclusions

New ΔP vs. Q measurements coupled with a previously reported U vs. ΔP database have resulted in new friction factor and heat transfer correlation equations for fan-driven impinging flow through square arrays of cylindrical cross-section pin-fins. The correlation equations include the effect of coolant flow rate, pin-fin density and pin-fin height. The equations exhibit the expected dynamical behavior when the fin density approaches the maximum fin density. Strictly speaking, these equations are limited to situations where air is the coolant and d/L = 0.05 and $d_f/L = 0.819$, $d_h/d_f = 0.519$ and $0.196 \le D \le 0.385$.

A comparison with jet-driven impingement on the same type of pin-fin arrays shows that the heat transfer / pressure drop characteristics of the two flow configurations are fundamentally different. When the same arrays are compared at the same coolant flow rate, the fan-driven configuration will result in a lower pressure drop and heat transfer rate. However, both correlations show that the heat transfer coefficient initially decreases with increase in fin density; a surprising result. An analysis shows that different optimal pin-fin configurations (fin height and fin density) result, depending on the design criteria imposed on the flow.

References

Sparrow, E. M. and Larson, E. D. (1982) "Heat Transfer from Pin-Fins situated in an Oncomming Longitudinal Flow which Turns to Crossflow" Int. J. Heat Mass Trans., Vol. 25, pp. 603 –614.

Wirtz, R.A., Sohal, R. and Wang, H. (1997) "Thermal Performance of Pin-Fin Fan-Sink Assemblies", Journal of Electronic Packaging, Vol. 119, pp.26-31.

Wirtz, R.A. and Zheng, N. (1998) "Methodology for Predicting Pin-Fin Fan-Sink Assembly Performance", Proceedings of 6th InterSociety Conference on Thermal and Thermomechanical Phenomena in Electronic Systems (Itherm'98), S. H. Bhavnani et al., ed., pp.303-309.

Zheng, N. (1998) Methodology for Predicting Pin-Fin Fan-Sink Assembly Performance, MS Thesis, Mechanical Engineering Department, University of Nevada, Reno, NV 89557.